Volume 92

2015

An NRC Research Press Journal

Une revue de NRC Research Press

www.nrcresearchpress.com

Canadian Journal of Physics

Revue canadienne de physique

In cooperation with the Canadian Association of Physicists

Avec le concours de l'Association canadienne des physiciens et physiciennes

NRC Research Press

NRC Research Press

ARTICLE

Hot plasma modes across Reissner–Nördstrom–de Sitter horizon in a Veselago medium

Ifra Noureen and Hafiza Rizwana Kausar

Abstract: We investigate wave attributes of hot plasma around a Reissner–Nördstrom–de Sitter (RN-dS) metric in a Veselago medium. A perturbation scheme is implemented on general relativistic magnetohydrodynamical (GRMHD) equations that are further used for Fourier analysis. The linearly perturbed Fourier-analyzed GRMHD equations depict the dispersion of hot plasma waves. It is found that inclusion of charge in de Sitter space greatly affects the wave dispersion. A comparison of wave properties is presented, and results reassert the presence of the Veselago medium.

PACS Nos.: 95.30.Sf, 95.30.Qd, 04.30.Nk.

Résumé : Nous étudions ici les caractéristiques ondulatoires des plasmas chauds autour d'une métrique de Reissner-Nördstrom-de Sitter (RN-dS) dans un milieu de Veselago. Nous implémentons un schéma perturbatif sur les équations de magnétohydrodynamique de relativité générale (GRMHD) qui sont utilisées ensuite pour une analyse de Fourier. Les équations d'analyse de Fourier à perturbation linéaire décrivent la dispersion d'ondes de plasma chaud. Nous observons que l'intrusion de charges dans l'espace de de Sitter a un effet important sur la dispersion des ondes. Nous présentons une comparaison des propriétés ondulatoires et les résultats vérifient la présence d'un milieu de Veselago. [Traduit par le Rédaction]

1. Introduction

Celestial objects, such as black hole (BH), are abundant in our universe. In a BH, gravitational pull is so stronger that nothing can escape from its so-called horizon. Relativists suggest that the death of massive stars or collapse of a supergiant star give birth to BHs. In 1916, Schwarzschild found the simplest BH as an exact solution of field equations [1].

Plasma is a distinct fourth state of matter, having positive and negatively charged particles, that potently interact with electromagnetic fields [2]. The theory of magnetohydrodynamics (MHD) is formulated for the study of plasma flow under the influence of magnetic fields. MHD in connection with gravitational effects is recognized as a distinct theory called general relativistic magnetohydrodynamics (GRMHD) [3]. An exact solution of the field equations for a charged object constitute the Reissner–Nördstrom spacetime. The de-Sitter metric is a vacuum solution of the field equations with a positive cosmological constant leading to the far future expanding universe [4–6].

The Reissner–Nördstrom–de Sitter (RN-dS) metric corresponds to spacetime solutions characterized by charge, mass, and cosmological constant that are assumed to be most pragmatic for astrophysical applications [7]. Regge and Wheeler [8], Zerilli [9], and Gleiser et al. [10] contributed to establish the stability of non-rotating BHs. ADM 3 + 1 formalism [11] is the most reliable approach for spacetime decomposition in general relativity, and it divides the metric into layers of three-dimensional space-like hypersurfaces and one-dimensional time. Petterson [12] concluded that the gravitational field is much stronger across the surface of a non-rotating BH.

Zhang [13] modified the laws of perfect GRMHD in general and also emphasized on stationary symmetric GRMHD solutions. He [14] also discussed rotating BH dynamics. Buzzi et al. [15] used ADM 3 + 1 split to characterize a two-fluid plasma with the help of two local approximations in the neighborhood of a Schwarzschild BH.

Astefanesei et al. [16] worked out RN-dS BHs in the context of a de-Sitter background to conformal field theory by using static and planar coordinates. Zhong and Gao [17] investigated particle collisions around cosmological horizon of a RN-dSsolution. Transverse wave propagation for a two-fluid plasma has also been determined for a Schwarzschild de-Sitter (SdS) magnetosphere [18]. Sharif and Sheikh [19, 20] analyzed plasma modes of cold and isothermal plasmas in the usual medium for non-rotating and rotating BHs. Sharif and Rafique [21] presented dispersion modes of a Schwarzschild horizon for the hot plasma in the usual medium.

Metamaterials are artificially produced materials with unusual electromagnetic properties, having enormous astrophysical applications. The Russian physicist Victor Veselago introduced such a metamaterial, named Veselago medium, that has a negative refractive index, permittivity, and permeability simultaneously [22]. Various scientists [23–27] analyzed negative phase velocity and the refractive index of such a metamaterial. Ziolkowski and Heyman [28] developed an analytic and numerical solution to establish wave properties of such a medium. Ramakrishna [29] explained the role of Veselago medium in perfect lensing phenomenon. After experimental realization of Veselago medium, plasma study in Veselago medium has gained enormous importance in recent years.

Sharif and Mukhtar [30] discussed dispersion relations for Schwarzschild horizon in unusual medium. Sharif and Noureen [31] determined dispersion modes of isothermal and hot plasma across SdS horizon for negative index medium. Recently, wave behavior around Reissner-Nördstrom spacetime was developed [32].

We also use ADM 3 + 1 split general line element,

Received 23 June 2014. Accepted 19 September 2014.

I. Noureen. Department of Mathematics, University of Management and Technology, 54000-Lahore, Pakistan.
H.R. Kausar. Department of Physics, University of Zurich, 8092-Zurich, Switzerland.
Corresponding author: Ifra Noureen (e-mail: ifra.noureen@gmail.com).

Published at www.nrcresearchpress.com/cjp on 13 October 2014.

Fig. 1. Dispersion is anomalous and waves are moving towards black hole horizon.

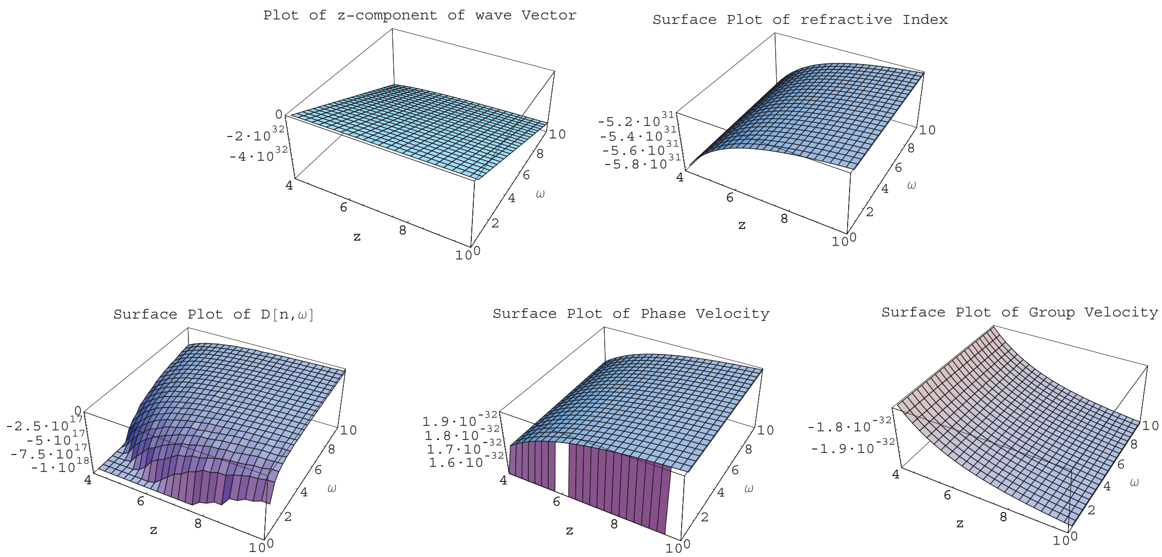

$$ds^2 = -\alpha^2 dt^2 + \eta_{mn}(dx^m + \beta^m dt)(dx^n + \beta^n dt) \tag{1.1}$$

where the lapse function (ratio of fiducial observer (FIDO), i.e., proper time to universal time, $d\tau/dt$) is expressed by α, β^m denotes shift vector in three dimensions, and components of space-like hypersurfaces are represented by η_{mn} (m, n = 1, 2, 3). In planar analogue of RN-dS spacetime $\alpha = \alpha(z)$, $\beta = 0$, $\eta_{mn} = 1$ ($m = n$), and so the metric becomes,

$$ds^2 = -\alpha^2(z)dt^2 + dx^2 + dy^2 + dz^2 \tag{1.2}$$

Wave analysis of hot plasma around RN-dS horizon in Veselago medium is examined in this paper. Since plasma is highly ionized, wave analysis of plasma around an expanding charged spacetime is very interesting. The paper is arranged as follows: Fourier-analyzed form of GRMHD equations for a rotating BH are given in Sect. 2. Section 3 provides numerical solutions of linearly perturbed Fourier-analyzed GRMHD equations for hot plasma. Comparison and summary is given in the last section.

2. Fourier-analyzed GRMHD equations in a Veselago medium

Here we use basic GRMHD equations (given in Appendix A) to obtain an insight into the Fourier-analyzed GRMHD equations. It is assumed that plasma flow is two dimensional, i.e., in xz-plane. Velocity $\boldsymbol{V}$ and magnetic field $\boldsymbol{B}$ measured by FIDO are,

$$\boldsymbol{V} = v(z)\mathrm{e}_x + u(z)\mathrm{e}_z \qquad \boldsymbol{B} = B[\xi(z)\mathrm{e}_x + \mathrm{e}_z] \tag{2.3}$$

Here B denotes constant. The relation between the quantities ξ, u, and v is [19],

$$v = \frac{C}{\alpha} + \xi u \tag{2.4}$$

where C represents a constant of integration. The Lorentz factor, $\gamma = 1/\sqrt{1-\boldsymbol{V}^2}$ turns out to be $\gamma = 1/\sqrt{1-u^2-v^2}$. To study the consequences of BH gravity on plasma, we implement a linear perturbation scheme to the flow variables (pressure p, mass density ρ, V and B) as follows:

$$\begin{aligned}\rho &= \rho^0 + \epsilon\rho = \rho^0 + \rho\tilde{\rho}\\ p &= p^0 + \epsilon p = p^0 + p\tilde{p}\\ \boldsymbol{V} &= \boldsymbol{V}^0 + \epsilon\boldsymbol{V} = \boldsymbol{V}^0 + \boldsymbol{v}\\ \boldsymbol{B} &= \boldsymbol{B}^0 + \epsilon\boldsymbol{B} = \boldsymbol{B}^0 + B\boldsymbol{b}\end{aligned} \tag{2.5}$$

where p, ρ^0, $\boldsymbol{V}^0$, and $\boldsymbol{B}^0$ represent the unperturbed quantities. The linearly perturbed quantities are denoted by $\epsilon\rho$, ϵp, $\epsilon\boldsymbol{V}$, and $\epsilon\boldsymbol{B}$. Dimensionless quantities $\tilde{\rho}$, $\tilde{p}$, v_x, v_z, b_x and b_z are used that corresponds to perturbed quantities,

$$\begin{aligned}&\tilde{p} = \tilde{p}(t,z) \qquad \tilde{\rho} = \tilde{\rho}(t,z)\\ &\boldsymbol{v} = \epsilon\boldsymbol{V} = v_x(t,z)\mathrm{e}_x + v_z(t,z)\mathrm{e}_z\\ &\boldsymbol{b} = \frac{\epsilon\boldsymbol{B}}{B} = b_x(t,z)\mathrm{e}_x + b_z(t,z)\mathrm{e}_z\end{aligned} \tag{2.6}$$

Application of linear perturbation in perfect GRMHD, (A1)–(A5), and insertion inoto (2.6) leads to a component form of linearly perturbed GRMHD equations [31], provided in the Appendix A. Further, to develop a Fourier analysis of perturbed GRMHD equations, metric dependence is considered in the following way,

$$\begin{aligned}&\tilde{\rho}(t,z) = a_1\mathrm{e}^{-\iota\omega t+\iota kz} \qquad \tilde{p}(t,z) = a_2\mathrm{e}^{-\iota\omega t+\iota kz}\\ &v_z(t,z) = a_3\mathrm{e}^{-\iota\omega t+\iota kz} \qquad v_x(t,z) = a_4\mathrm{e}^{-\iota\omega t+\iota kz}\\ &b_z(t,z) = a_5\mathrm{e}^{-\iota\omega t+\iota kz} \qquad b_x(t,z) = a_6\mathrm{e}^{-\iota\omega t+\iota kz}\end{aligned} \tag{2.7}$$

where k is the z-component of the wave vector (wave number), and angular frequency is expressed by ω. To find the refractive index and other plasma properties, we use the above wave number. Here dispersion corresponding to the effects of frequency dependence during wave propagation. Insertion into (2.7) and the component form of the linearly perturbed GRMHD equations leads to the Fourier-analyzed form,

$$a_4(\alpha' + \iota k\alpha) - a_3[(\alpha\xi)' + \iota k\alpha\xi] - a_5(\alpha v)' - a_6[(\alpha u)' + \iota\omega + \iota ku\alpha] = 0 \tag{2.8}$$

$$a_5\left(\frac{-\iota\omega}{\alpha}\right) = 0 \tag{2.9}$$

Fig. 2. Waves move away from horizon but disperse anomalously.

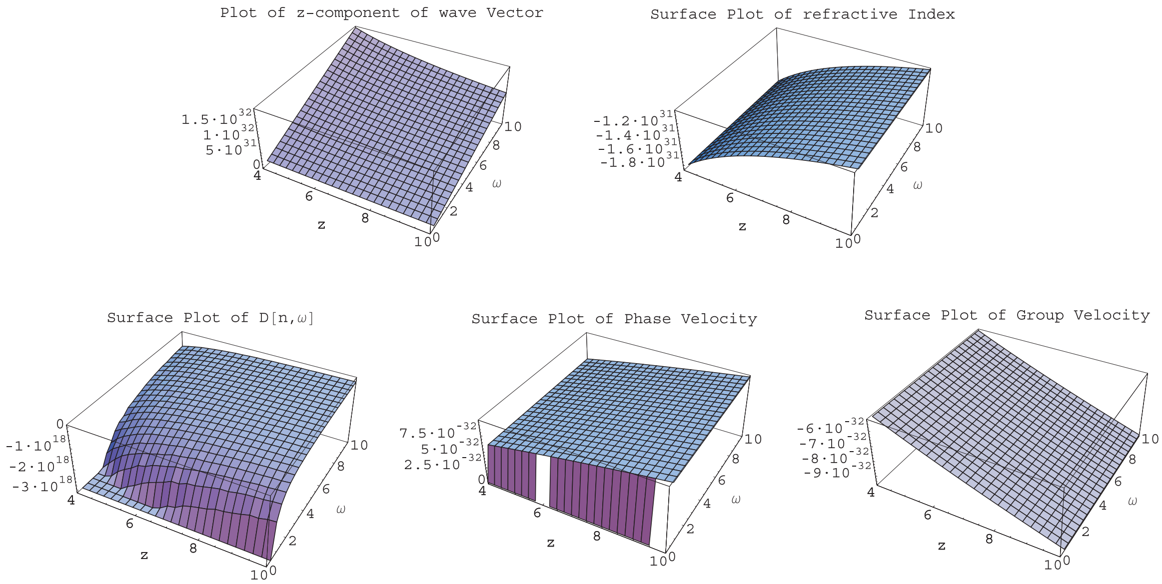

Fig. 3. Normal dispersion with the waves in direction of the horizon.

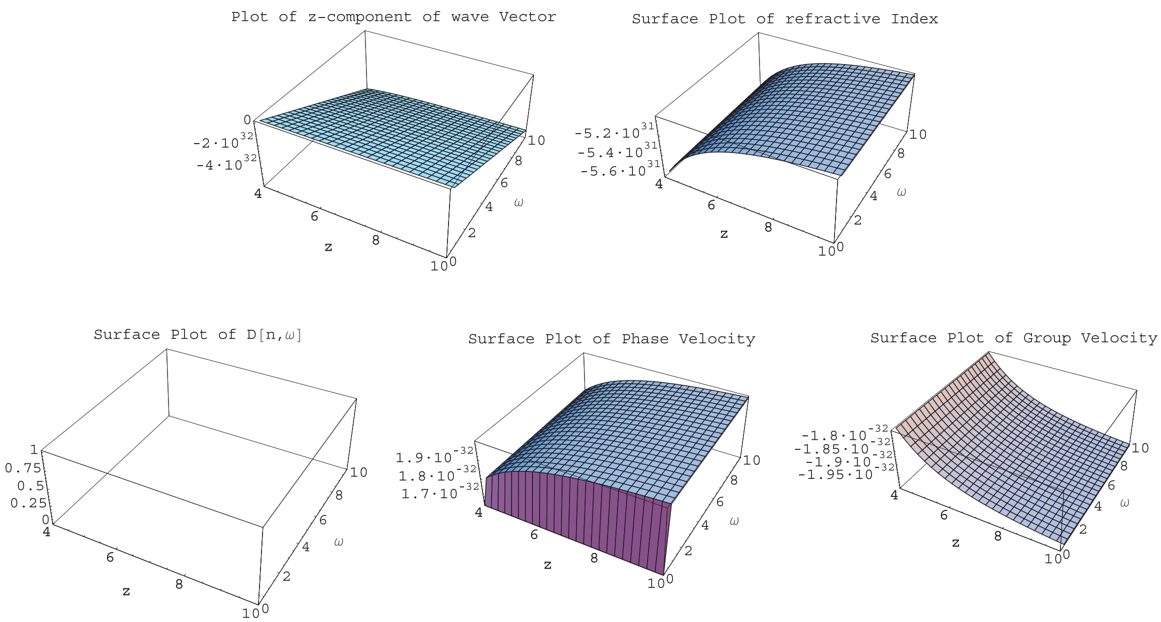

$$a_5 \iota k = 0 \tag{2.10}$$

$$a_1\left(\frac{-\iota\omega}{\alpha}\rho\right) + a_2\left(\frac{-\iota\omega}{\alpha}p\right) + a_3(\rho + p)\left[\frac{-\iota\omega}{\alpha}\gamma^2 u + (1 + \gamma^2u^2)\iota k - (1 - 2\gamma^2u^2)(1 + \gamma^2u^2)\frac{u'}{u} + 2\gamma^4u^2vv'\right] + a_4(\rho + p)\gamma^2 \times \left[\left(\frac{-\iota\omega}{\alpha} + \iota ku\right)v + u(1 + 2\gamma^2v^2)v' + 2\gamma^2u^2vu'\right] = 0 \tag{2.11}$$

Table 1. Dispersion and direction of waves.

In direction of horizon	Figs. 1, 3
Moving away from horizon	Fig. 2
Normal dispersion	Fig. 3
Anomalous dispersion	Figs. 1, 2
Increasing n with increasing z	Fig. 1, $4.3 \le z \le 7.9$, $0 \le \omega \le 9$
	Fig. 2, $4 \le z \le 9.2$, $0 \le \omega \le 10$
	Fig. 3, $7.5 \le z \le 9$, $1 \le \omega \le 8$

Fig. 4. Normal dispersion is observed but waves are moving towards the horizon.

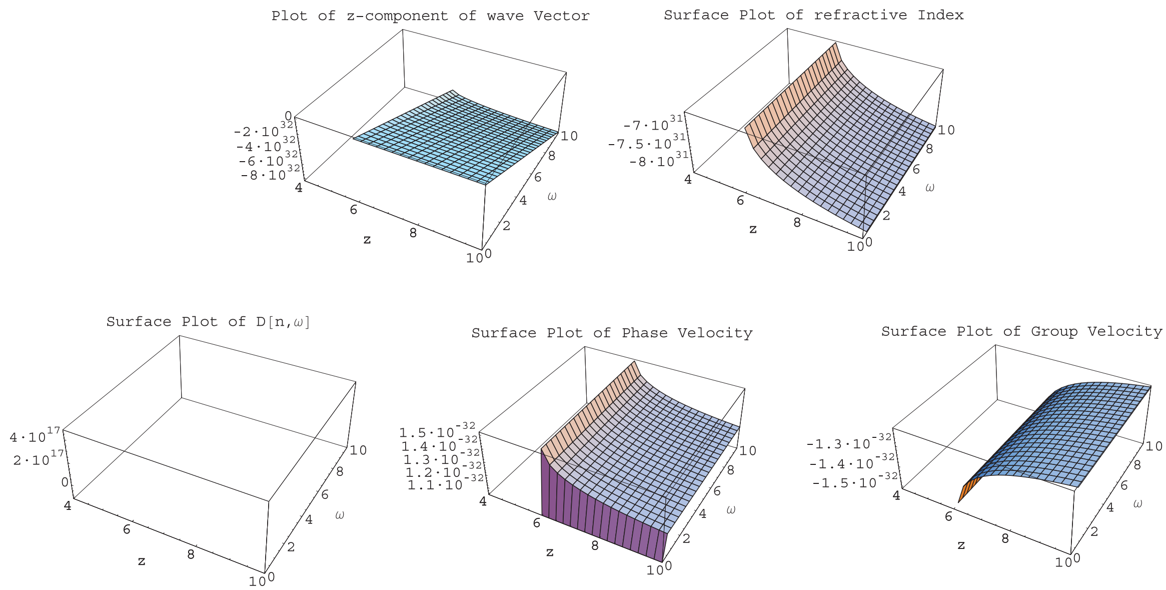

$$a_1\{\rho\gamma^2 u[(1+\gamma^2v^2)v' + \gamma^2 v u u'] + \gamma^2 v u(\rho' + \iota k\rho)\} + a_2\{p\gamma^2 u \times [(1+\gamma^2v^2)v' + \gamma^2 vuu'] + \gamma^2 vu(p' + \iota k p)\} + a_3\Big\{(\rho+p)\gamma^2\Big[(1+2\gamma^2u^2)(1+2\gamma^2v^2)v' + \left(\frac{-\iota\omega}{\alpha}+\iota k u\right)\gamma^2 vu - \gamma^2v^2v' + 2\gamma^2(1+2\gamma^2u^2)uvu'\Big] + \gamma^2 v(1+2\gamma^2u^2)(\rho'+p') - \frac{B^2u}{4\pi\alpha}(\xi\alpha)' + \frac{\xi B^2}{4\pi}\left(\frac{\iota\omega}{\alpha} - \iota k u\right)\Big\} + a_4\Big\{(\rho+p)\gamma^4 u[(1+4\gamma^2v^2)uu' + 4vv'(1+\gamma^2v^2)] + (\rho+p)\gamma^2(1+\gamma^2v^2)\left(\frac{-\iota\omega}{\alpha}+\iota k u\right) + \gamma^2 u(1+2\gamma^2v^2)(\rho'+p') + \frac{B^2}{4\pi}\left(\frac{u\alpha'}{\alpha}\frac{\iota\omega}{\alpha} + \iota k u\right)\Big\} - a_6\frac{B^2}{4\pi\alpha}\{\alpha u u' + \alpha'(1+u^2) + (1+u^2)\iota k\alpha\} = 0 \tag{2.12}$$

$$a_1\{\rho\gamma^2[a_z + (1+\gamma^2u^2)uu' + \gamma^2u^2vv'] + \gamma^2u^2(\rho'+\iota k\rho)\} + a_2\{p\gamma^2[a_z + (1+\gamma^2u^2)uu' + \gamma^2u^2vv'] + (1+\gamma^2u^2)(p'+\iota k p)\} + a_3\Big((\rho+p)\gamma^2\Big\{(1+\gamma^2u^2)\left(\frac{-\iota\omega}{\alpha}+\iota k u\right) + u'(1+\gamma^2u^2)(1+4\gamma^2u^2) + 2u\gamma^2[a_z + (1+2\gamma^2u^2)\times vv']\Big\} + 2\gamma^2u(1+\gamma^2u^2)(\rho'+p') + \frac{\xi B^2 u}{4\pi\alpha}(\xi\alpha)' - \frac{\xi^2B^2}{4\pi}\left(\frac{\iota\omega}{\alpha} - \iota k u\right)\Big) + a_4\Big((\rho+p)\gamma^4\Big\{\left(\frac{-\iota\omega}{\alpha}+\iota k u\right)uv + u^2v'(1+4\gamma^2v^2) + 2v[a_z + (1+2\gamma^2u^2)uu']\Big\} + 2\gamma^4u^2v(\rho'+p') + \frac{\xi B^2}{4\pi}\left(\frac{\iota\omega}{\alpha}-\iota k u\right) - \frac{\xi B^2 u\alpha'}{4\pi\alpha}\Big) + a_6\Big\{\frac{B^2}{4\pi\alpha}[-(\xi\alpha)' + \alpha'\xi - u\xi(u\alpha' + u'\alpha)] + \frac{\xi B^2}{4\pi}(1+u^2)\iota k\Big\} = 0 \tag{2.13}$$

$$a_1\left[\left(\frac{-\iota\omega}{\alpha}\gamma^2 + \iota k u\gamma^2 + 2u\gamma^2 a_z + \gamma^2 u'\right)\rho + u\rho'\gamma^2\right] + a_2\left\{\left[\frac{\iota\omega}{\alpha}(1-\gamma^2) + \iota k u\gamma^2 + 2\gamma^2 u a_z + \gamma^2 u'\right]p + u\gamma^2 p'\right\} + a_3\gamma^2\Big[(\rho'+p') + 2(2\gamma^4 uu' + a_z + 2\gamma^2u^2a_z)(\rho+p) + (1+2\gamma^2u^2)(\rho+p)\iota k + \frac{\xi B^2}{4\pi\alpha}(\xi u - v)\iota\omega + \alpha\xi'\Big] + a_4\Big\{2(\rho+p)\gamma^2[(uv' + 2uva_z + u'v) + uv\iota k] + \frac{B^2}{4\pi\alpha}(v - u\xi)\iota\omega - \alpha\xi'\Big\} + a_6\Big\{\frac{-B^2}{4\pi\alpha}[(v^2+u^2)\xi + \xi v(\xi v + u)\iota\omega] - \alpha\xi' u + \iota k\alpha(v - u\xi)\Big\} = 0 \tag{2.14}$$

3. Hot plasma dispersion modes

The equation of state is used to obtain the numerical solution of Fourier-analyzed form for a rotating environment. For hot plasma, it is given by [13],

$$\mu = \frac{\rho + p}{\rho_0} \tag{3.15}$$

The specific enthalpy μ in (3.15) is non-constant, and so affects the perturbed GRMHD eqs. (2.8)–(2.14) for hot plasma around the RN-dS BH horizon. In the following subsections, we discuss the hot plasma case in the magnetized and non-magnetized backgrounds.

3.1. Non-magnetized background

In non-magnetized environment, $B = 0 = \xi$ leads to $a_5 = 0 = a_6$, in the Fourier-analyzed GRMHD eqs. (2.11)–(2.14) [31]. To solve the Fourier-analyzed equations numerically, we assume,

$$\mu = \sqrt{\frac{1+\alpha^2}{2}} \qquad \rho = p = \frac{\mu}{2} \qquad \alpha = \frac{z}{2r} \qquad r = r_+ + r_h$$

with

Fig. 5. Anomalous dispersion with waves in the direction of the event horizon.

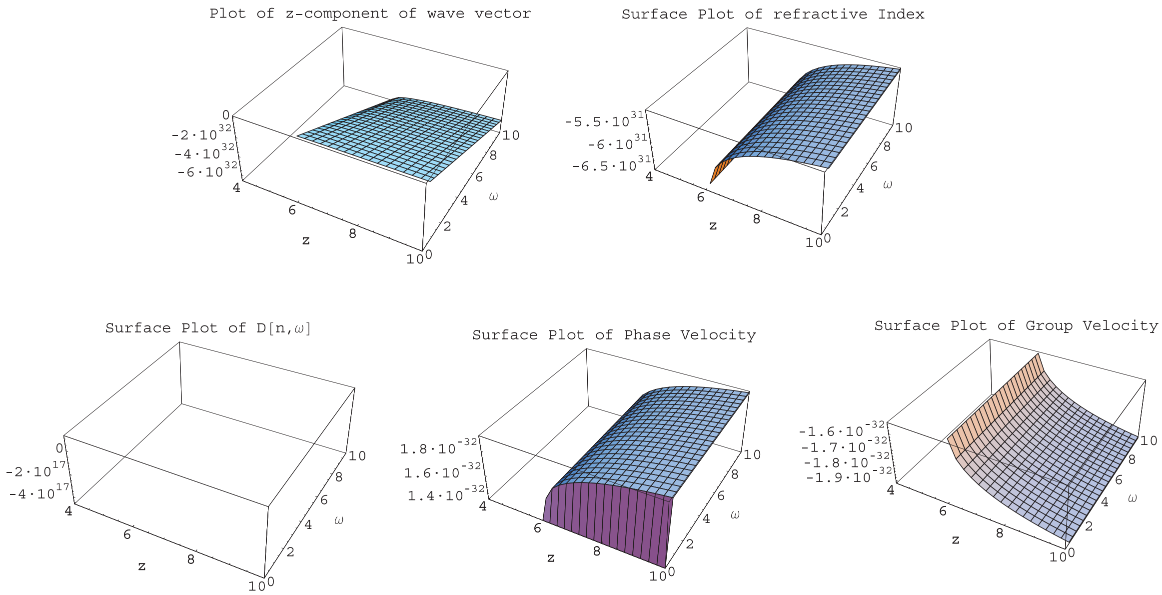

Fig. 6. Waves are directed towards the horizon and disperse normally.

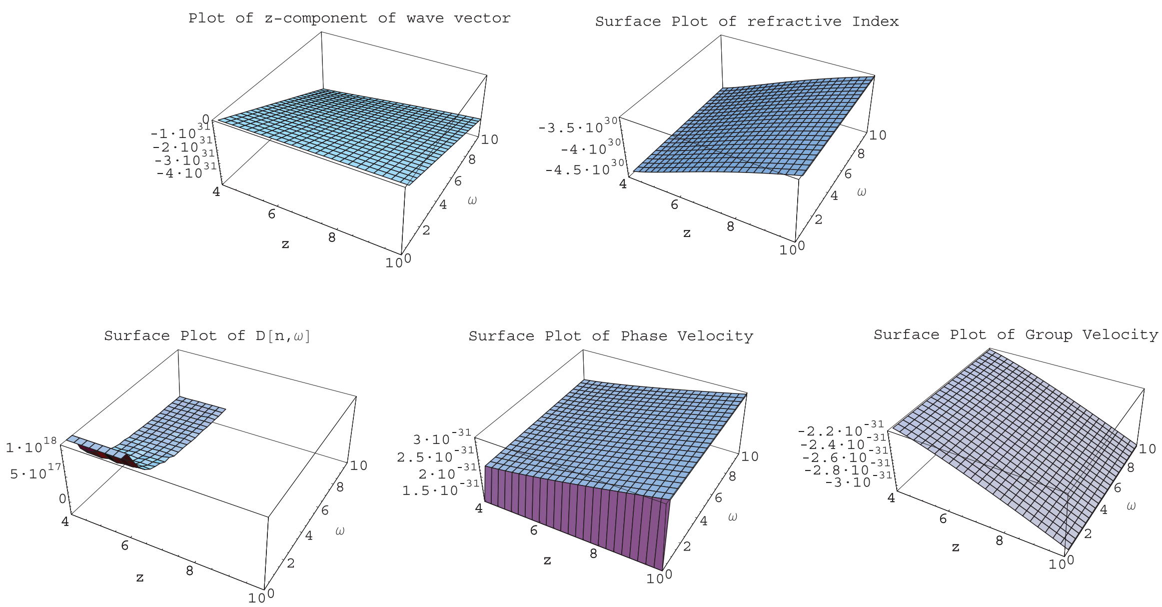

$$r_+ = \frac{z}{2(M + \sqrt{M^2 + Q^2})} \qquad \frac{Q^2}{M^2} = 0.7 \qquad u = v = -\frac{1}{\sqrt{z^2 + 2}}$$

and

$$\gamma = \frac{1}{\sqrt{1 - u^2 - v^2}} = \frac{\sqrt{z^2 + 2}}{z}$$

where

$$r_h \approx 2M\left(1 + \frac{4M^2}{l^2} + \ldots\right) \simeq \zeta 2.948 \text{ km} \quad 1 \leq \zeta \leq 1.5$$

and $M \sim 1M_\odot$ [18].

The region under consideration is $4 \leq z \leq 10$ with event horizon at $z = 0$. The region $0 \leq z \leq 4$ is ignored, because wave propagation cannot be viewed graphically and results are not interesting in this region. A dispersion relation is formed from the determinant of coefficients of the corresponding Fourier-analyzed equations for non-magnetized plasma. The real part of the dispersion relation evolve quartic equation in k, is given as,

$$H_1(z)k^4 + H_2(z, \omega)k^3 + H_3(z, \omega)k^2 + H_4(z, \omega)k + H_5(z, \omega) = 0 \qquad (3.16)$$

which has 2 real and 2 imaginary roots. The imaginary part of dispersion relation is cubic in k,

Fig. 7. The interesting case: normal and anomalous dispersion at random points in the region along with waves moving away from the horizon.

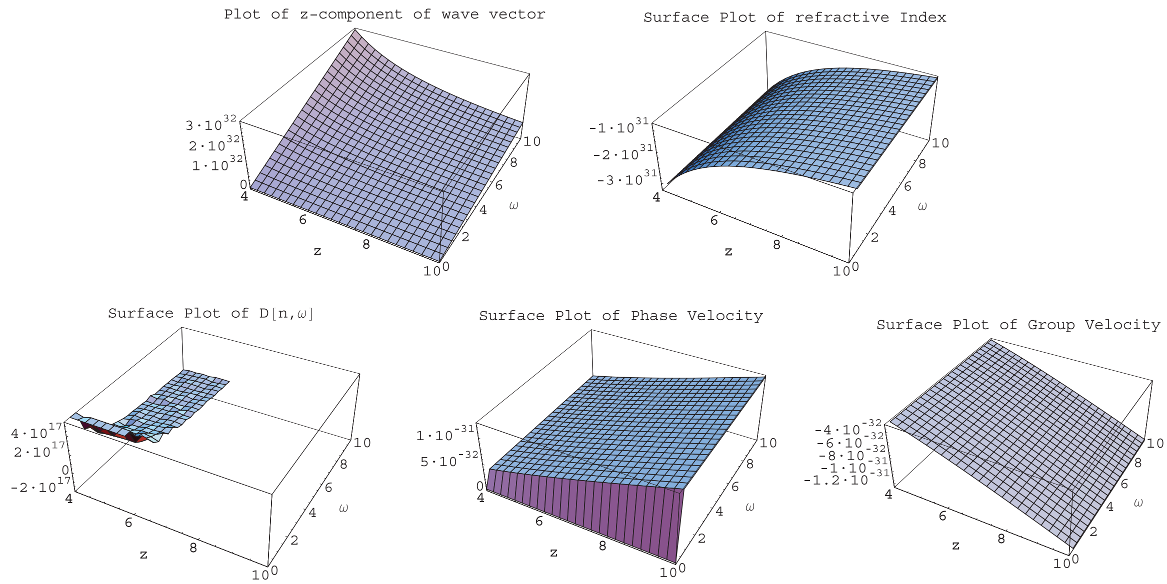

Fig. 8. Waves exhibit normal and anomalous dispersion and moving towards the horizon.

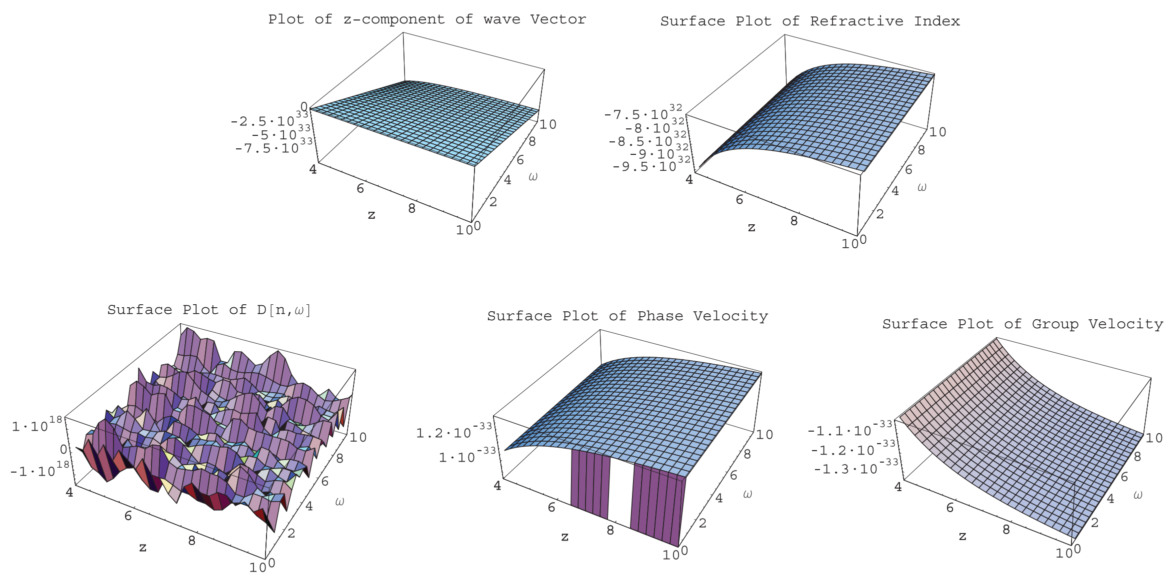

$$D_1(z)k^3 + D_2(z,\omega)k^2 + D_3(z,\omega)k + D_4(z,\omega) = 0 \tag{3.17}$$

which has 1 real and 2 complex roots.

The wave number k can be used to obtain the refractive index, whose change $dn/d\omega$ determines whether the dispersion is anomalous or normal, which is the equivalent of saying that the region where the phase velocity is greater than the group velocity corresponding to normal dispersion, otherwise anomalous [33]. Wave phenomenon around an event horizon can be beneficial only for those values of k for which waves propagate in opposite direction of the horizon and dispersion is normal. However, no information can be extracted about the magnetosphere for waves that disperse anomalously.

We mention here that dispersion relations are solved by using Mathematica software. There are a few roots for which change in refractive index does not show a three-dimensional plot, but those values are shown on axis. Some complicated expressions that Mathematica could not plot on a graph is the cause.

Figures 1–3 provide three-dimensional views of wave properties of non-magnetized hot plasma around the RN-dS horizon, with further explanations in Table 1.

3.2. Plasma flow in magnetized background

For rotating magnetized plasma flow, the perturbed Fourier-analyzed GRMHD equations are given by (2.8)–(2.14). In this case, flow is two dimensional, hence $\boldsymbol{V}$ and $\boldsymbol{B}$ lie in the xz-plane. For numerical solutions, velocity, lapse function, and specific enthalpy are the same as for non-magnetized background. Here, magnetic field is assumed to be $B^2/4\pi = 2$ with $u = v$. By putting $C = 1$ in (2.4), we obtain $\xi = 1 + \sqrt{2 + z^2}/z$. The region for wave analysis is set to $4 \le z \le 10$ and $0 \le \omega \le 10$, and in this case (2.9)–(2.10) yield

Fig. 9. Normal and anomalous dispersion but waves are moving towards the horizon.

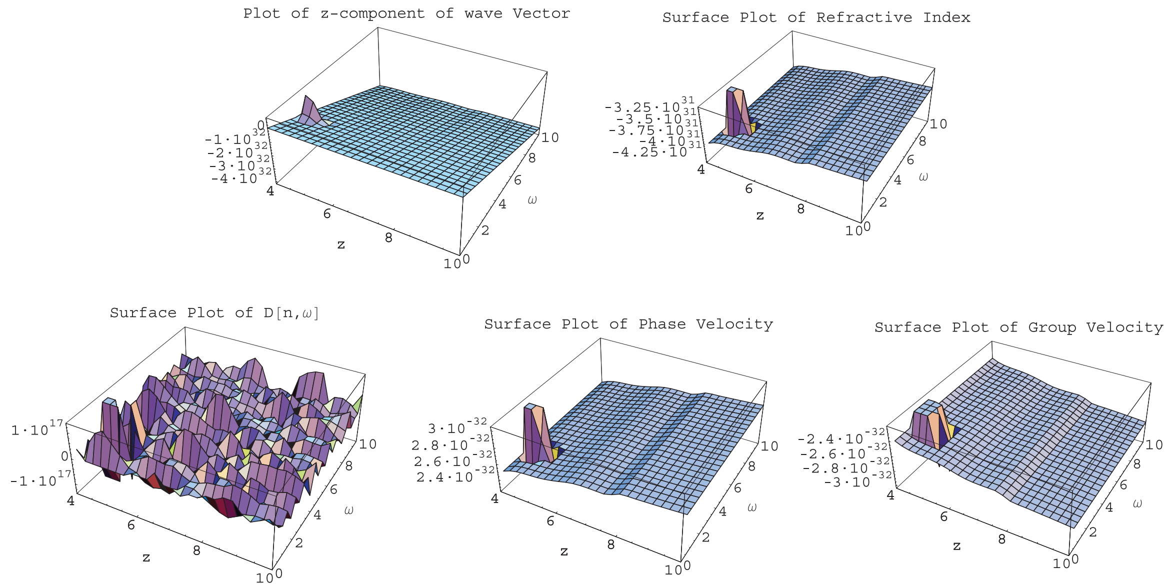

Fig. 10. Normal and anomalous dispersion randomly with waves in opposite direction to the horizon, implying energy extraction information.

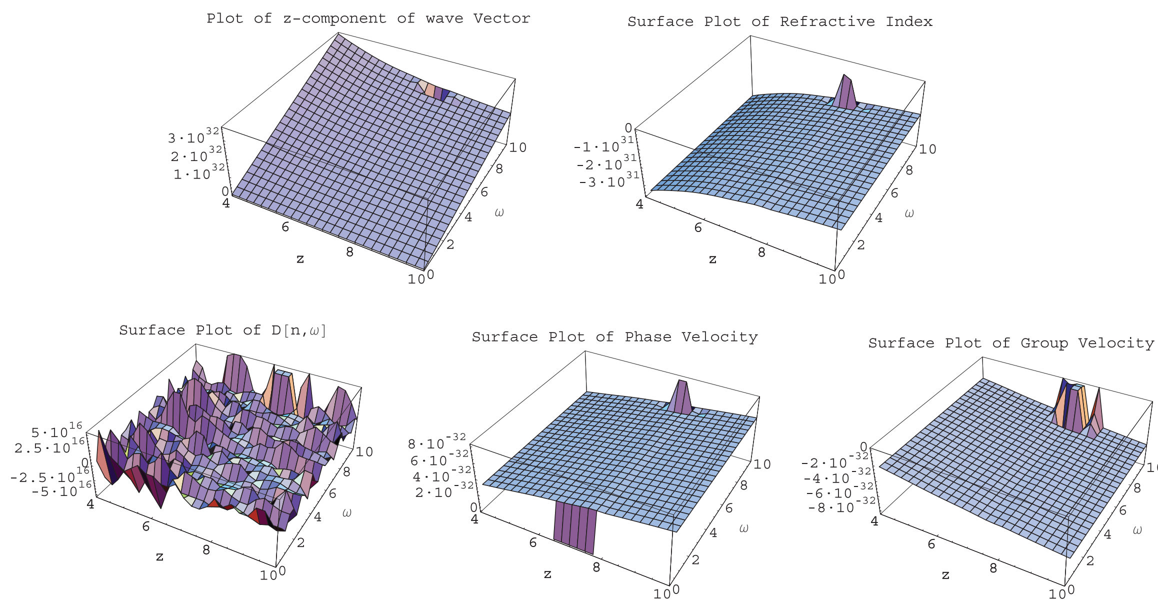

$a_5 = 0$. The determinant of the Fourier-analyzed form generates a dispersion relation whose real part is,

$$D_1(z)k^4 + D_2(z,\omega)k^3 + D_3(z,\omega)k^2 + D_4(z,\omega)k + D_5(z,\omega) = 0 \qquad (3.18)$$

which as 4 real roots as shown in Figs. 4–7. The imaginary part is given by,

$$E_1(z)k^5 + E_2(z,\omega)k^4 + E_3(z,\omega)k^3 + E_4(z,\omega)k^2 + E_5(z,\omega)k + E_6(z,\omega) = 0 \qquad (3.19)$$

which yields 3 real and 2 complex roots, as shown in Figs. 8–10. The plasma modes for magnetized background are tabulated in Tables 2 and 3.

Table 2. Refractive index and direction of waves.

In direction of horizon	Figs. 4, 5, 6, 8, 9
Moving away from horizon	Figs. 7, 10
Normal dispersion	Fig. 4
Anomalous dispersion	Fig. 5
Increasing n with increasing z	Fig. 5, $6.1 \le z \le 9.9$, $1 \le \omega \le 8$
	Fig. 6, $4.6 \le z \le 8.6$, $1 \le \omega \le 9.6$
	Fig. 7, $4 \le z \le 8.2$, $0 \le \omega \le 9$
	Fig. 8, $4.3 \le z \le 9.4$, $1 \le \omega \le 9$
	Fig. 10, $4 \le z \le 6.8$, $1 \le \omega \le 9$
Decreasing n with increasing z	Fig. 4, $5.7 \le z \le 10$, $0 \le \omega \le 4$
	Fig. 9, $4.3 \le z \le 4.9$, $1.3 \le \omega \le 9.1$

Table 3. Normal and anomalous dispersion regions.

Fig.	Normal dispersion	Anomalous dispersion
7	$4 \le z \le 5.1$, $4 \le \omega \le 6$	$4.9 \le z \le 5.3$, $0 \le \omega \le 1.7$
8	$8.1 \le z \le 8.9$, $1.5 \le \omega \le 3.1$	$4.3 \le z \le 5.1$, $7 \le \omega \le 8.3$
9	$5.3 \le z \le 5.4$, $1.8 \le \omega \le 1.9$	$5.1 \le z \le 5.7$, $7 \le \omega \le 8$
	$4.1 \le z \le 4.4$, $1.5 \le \omega \le 3$	$7 \le z \le 7.9$, $0.5 \le \omega \le 1.1$
10	$7 \le z \le 7.7$, $4.2 \le \omega \le 4.9$	
	$4 \le z \le 4.4$, $7 \le \omega \le 7.7$	$8 \le z \le 8.6$, $9.2 \le \omega \le 9.4$
12		$4 \le z \le 4.3$, $0 \le \omega \le .3$

4. Summary

We investigated hot plasma modes around the RN-dS horizon in the presence of Veselago medium. We rewrote perfect GRMHD equations in Veselago medium by implementing ADM formalism. Plasma flow distorts due to gravitational and electromagnetic effects of charged BHs (RN-dS). Linear perturbation is applied on flow variables to investigate the gravitional effects of a BH. Moreover, it is assumed that plasma flow is two-dimensional, i.e., in the *xz*-plane. Dimensionless quantities corresponding to flow variables are introduced to build component forms of linearly perturbed GRMHD equations.

The technique of Fourier analysis is applied to form dispersion relations for the rotating (non-magnetized and magnetized) plasma. Non-magnetized hot plasma indicates that waves in Figs. 1 and 3 are directed towards the BH horizon and move away from the horizon in Fig. 2. The dispersion is anomalous throughout the region in Figs. 1 and 2, whereas it is normal in Fig. 3.

In a magnetized environment, waves are in the direction of the event horizon in Figs. 4–6 and 8–9, while they move away from the horizon in Figs. 7 and 10. Normal as well as anomalous dispersion is observed in Figs. 7–10, while it is anomalous in Fig. 5 and normal in Figs. 4 and 6.

In conventional refraction, n is always greater than one. However, it is negative for a Veselago medium. Phase velocity should be greater than group velocity in an unusual medium, and so in all the figures, the refractive index is less than one. The refractive index increases and decreases in small regions, and the dispersion is normal when $dn/d\omega$ is positive and anomalous otherwise. All the roots of the dispersion relation in non-magnetize and magnetized plasmas satisfy unusual properties of the Veselago medium. The results reassert the presence of such an unusual medium in RN-dS magnetosphere.

It follows from previous work [31] that inclusion of a positive cosmological constant in non-rotating BH may reveal more information about the magnetosphere. Here we have inspected that addition of charge along with cosmological constant reveals anomalous dispersion at a majority of points in the region, however most of the waves move towards the event horizon. It may be concluded that spacetime charge affects the electromagnetic field firmly and that waves are directed towards BH horizon.

Previous work [30, 31] on plasma wave properties of non-rotating BHs, including Schwarzschild and SdS horizon, presents the fact that energy extraction information withdrawal is more effective in the case of de-Sitter space. On comparison with recent work [32] on waves around the RN horizon, it was observed that the addition of a cosmological constant to charged BH, i.e., RN-dS spacetime, provides more interesting results in terms of energy extraction around a magnetosphere. Hot plasma is a more generalized form of plasma, and it is reducible to an isothermal plasma when specific enthalpy is considered to be constant.

References

1. M. Camenzind. Compact objects in astrophysics: white dwarfs, neutron stars and black holes. Springer, Berlin. 2007. 682 p.
2. W. Baumjohann and R.A. Treumann. Basic space plasma physics. Imperial College Press, London. 1997.
3. D. Raine and E. Thomas. Black holes: an introduction. Imperial College Press, London. 2005.
4. A.G. Reiss, A.V. Filippenko, P. Challis, et al. Astron. J. **116**, 1009 (1998). doi:10.1086/300499.
5. N.A. Bahcall, J.P. Ostriker, S. Perlmutter, and P.J. Steinhardt. Science, **284**, 1481 (1999). doi:10.1126/science.284.5419.1481.
6. S. Perlmutter, G. Aldering, S. Deustua, et al. Bull. Am. Astron. Soc. **29**, 85.04 (1997). arXiv:astro-ph/9812473.
7. D.R. Brill and S.A. Hayward. Class. Quantum Grav. **11**, 359 (1994). doi:10.1088/0264-9381/11/2/008.
8. T. Regge and J.A. Wheeler. Phys. Rev. **108**, 1063 (1957). doi:10.1103/PhysRev.108.1063.
9. F.J. Zerilli. Phys. Rev. D, **2**, 2141 (1970). doi:10.1103/PhysRevD.2.2141; J. Math. Phys. **11**, 2203 (1970). doi:10.1063/1.1665380; Phys. Rev. Lett. **24**, 737 (1970). doi:10.1103/PhysRevLett.24.737.
10. R.J. Gleiser, C.O. Nicasio, R.H. Price, and J. Pullin. Class. Quantum Grav. **13**, L117 (1996). doi:10.1088/0264-9381/13/10/001.
11. R. Arnowitt, S. Deser, and C.W. Misner. *In* Gravitation: an introduction to current research. *Edited by* L. Witten. John Wiley, New York. pp. 227–264. 1962.
12. J.A. Petterson. Phys. Rev. D, **10**, 3166 (1974). doi:10.1103/PhysRevD.10.3166.
13. X.-H. Zhang. Phys. Rev. D, **39**, 2933 (1989). doi:10.1103/PhysRevD.39.2933.
14. X.-H. Zhang. Phys. Rev. D, **40**, 3858 (1989). doi:10.1103/PhysRevD.40.3858.
15. V. Buzzi, K.C. Hines, and R.A. Treumann. Phys. Rev. D, **51**, 6663 (1995). doi:10.1103/PhysRevD.51.6663; ibid. 6677. doi:10.1103/PhysRevD.51.6677.
16. D. Astefanesei, R. Mann, and E. Radu. JHEP, 2004(01), 029 (2004). doi:10.1088/1126-6708/2004/01/029.
17. C. Zhong and S. Gao. JETP Lett, **94**, 589 (2011). doi:10.1134/S0021364011200161.
18. M.H. Ali and M.A. Rahman. Int. J. Theor. Phys. **48**, 1717 (2009). doi:10.1007/s10773-009-9946-8.
19. M. Sharif and U. Sheikh. Gen. Relativ. Gravit. **39**, 1437 (2007). doi:10.1007/s10714-007-0465-8; ibid. 2095. doi:10.1007/s10714-007-0505-4; Int. J. Mod. Phys. A, **23**, 1417 (2008). doi:10.1142/S0217751X0803855X; J. Korean Phys. Soc. **52**, 152 (2008). doi:10.3938/jkps.52.152; **53**, 2198 (2008). doi:10.3938/jkps.53.2198.
20. M. Sharif and U. Sheikh. Class. Quantum Grav. **24**, 5495 (2007). doi:10.1088/0264-9381/24/22/013; Can. J. Phys. **87**, 879 (2009). doi:10.1139/P09-025; J. Korean Phys. Soc. **55**, 1677 (2009). doi:10.3938/jkps.55.1677.
21. M. Sharif and A. Rafique. Astrophys. Space Sci. **325**, 227 (2010). doi:10.1007/s10509-009-0183-7.
22. V.G. Veselago Sov. Phys. Usp. **10**, 509 (1968). doi:10.1070/PU1968v010n04ABEH003699.
23. D.R. Smith and N. Kroll. Phys. Rev. Lett. **85**, 2933 (2000). doi:10.1103/PhysRevLett.85.2933. PMID:11005971.
24. A. Lakhtakia, M.W. McCall, W.S. Weiglhofer, J. Gerardin, and J. Wang. Arch. Elektr. Ueber. **56**, 407 (2002).
25. K.Y. Bliokh and Y.P. Bliokh. Physics-Uspekhi. **47**, 393 (2004). doi:10.1070/PU2004v047n04ABEH001728.
26. T.G. Mackay and A. Lakhtakia. Current Sci. **90**, 640 (2006).
27. P.M. Valanju, R.M. Walser, and A.P. Valanju. Phys. Rev. Lett. **88**, 187401 (2002). doi:10.1103/PhysRevLett.88.187401. PMID:12005718.
28. R.W. Ziolkowski and E. Heyman. Phys. Rev. E, **64**, 056625 (2001). doi:10.1103/PhysRevE.64.056625.
29. S.A. Ramakrishna. Rep. Prog. Phys. **68**, 449 (2005). doi:10.1088/0034-4885/68/2/R06.
30. M. Sharif and N. Mukhtar. Astrophys. Space Sci. **331**, 151 (2011). doi:10.1007/s10509-010-0430-y; ibid. **333**, 187 (2011). doi:10.1007/s10509-011-0594-0.
31. M. Sharif and I. Noureen. Astrophys. Space Sci. **340**, 185 (2012). doi:10.1007/s10509-012-1022-9; Can. J. Phys. **89**, 991 (2011). doi:10.1139/p11-071.
32. M.H. Ali and M.A. Khan. Astrophys. Space Sci. **348**, 163 (2013). doi:10.1007/s10509-013-1538-7.
33. J.D. Achenbach. Wave propagation in elastic solids. North-Holland Publishing Company, Amsterdam. 1973.

Appendix A

The GRMHD equations are determined from basic MHD equations according to Maxwell's electrodynamical equations. 3 + 1 GRMHD equations for RN-dS metric in a Veselago medium become [31],

$$\frac{\partial \boldsymbol{B}}{\partial t} = -\nabla \times (\alpha \boldsymbol{V} \times \boldsymbol{B}) \tag{A1}$$

$$\nabla \cdot \boldsymbol{B} = 0 \tag{A2}$$

$$\frac{\partial(\rho + p)}{\partial t} + (\rho + p)\left[\gamma^2 \boldsymbol{V} \cdot \frac{\partial \boldsymbol{V}}{\partial t} + \gamma^2 \boldsymbol{V} \cdot (\alpha \boldsymbol{V} \cdot \nabla)\boldsymbol{V} + \nabla \cdot (\alpha \boldsymbol{V})\right] = 0 \tag{A3}$$

$$\left[\left((\rho + p)\gamma^2 + \frac{\boldsymbol{B}^2}{4\pi}\right)\delta_{ij} + (\rho + p)\gamma^4 V_i V_j - \frac{1}{4\pi}B_i B_j\right]\left(\frac{1}{\alpha}\frac{\partial}{\partial t} + \boldsymbol{V}\cdot\nabla\right)V^j + \gamma^2 V_i(\boldsymbol{V}\cdot\nabla)(\rho + p) - \left(\frac{\boldsymbol{B}^2}{4\pi}\delta_{ij} - \frac{1}{4\pi}B_i B_j\right)V^j_{,k}V^k$$
$$= -(\rho + p)\gamma^2 a_i - p_{,i} + \frac{1}{4\pi}(\boldsymbol{V}\times\boldsymbol{B})_i\nabla\cdot(\boldsymbol{V}\times\boldsymbol{B}) - \frac{1}{8\pi\alpha^2}(\alpha\boldsymbol{B})^2_{,i} + \frac{1}{4\pi\alpha}(\alpha B_i)_{,j}\boldsymbol{B}^j - \frac{1}{4\pi\alpha}(\boldsymbol{B}\times\{\boldsymbol{V}\times[\nabla\times(\alpha\boldsymbol{V}\times\boldsymbol{B})]\})_i \quad (A4)$$

$$-\frac{1}{\alpha}\frac{\partial p}{\partial t} + (\rho + p)\left[\left(\frac{1}{\alpha}\frac{\partial}{\partial t} + \boldsymbol{V}\cdot\nabla\right)\gamma^2 + 2\gamma^2(\boldsymbol{V}\cdot\boldsymbol{a}) + \gamma^2(\nabla\cdot\boldsymbol{V})\right]$$
$$- \frac{1}{4\pi\alpha}(\boldsymbol{V}\times\boldsymbol{B})\cdot\left[\left(\boldsymbol{V}\times\frac{\partial\boldsymbol{B}}{\partial t}\right) + \left(\boldsymbol{B}\times\frac{\partial\boldsymbol{B}}{\partial t}\right) - (\nabla\times\alpha\boldsymbol{B})\right] = 0 \quad (A5)$$

The component form of the linearly perturbed GRMHD equation takes following form,

$$\frac{1}{\alpha}\frac{\partial b_x}{\partial t} - ub_{x,z} = (ub_x - vb_z - v_x + \lambda v_z)\nabla\ln\alpha$$
$$- (v_{x,z} - \lambda v_{z,z} - \lambda' v_z + v' b_z + vb_{z,z} - u' b_x) \quad (A6)$$

$$\frac{1}{\alpha}\frac{\partial b_z}{\partial t} = 0 \quad (A7)$$

$$b_{z,z} = 0 \quad (A8)$$

$$\rho\frac{1}{\alpha}\frac{\partial\tilde{\rho}}{\partial t} + p\frac{1}{\alpha}\frac{\partial\tilde{p}}{\partial t} + (\rho + p)\gamma^2 v\left[\frac{1}{\alpha}\frac{\partial v_x}{\partial t} + uv_{x,z}\right] + (\rho + p)\gamma^2 u\frac{1}{\alpha}\frac{\partial v_z}{\partial t}$$
$$+ (\rho + p)(1 + \gamma^2u^2)v_{z,z} = -\gamma^2 u(\rho + p)[(1 + 2\gamma^2v^2)v' + 2\gamma^2uvu']v_x$$
$$+ (\rho + p)\left[(1 - 2\gamma^2u^2)(1 + \gamma^2u^2)\frac{u'}{u} - 2\gamma^4u^2vv'\right]v_z \quad (A9)$$

$$\left[(\rho + p)\gamma^2(1 + \gamma^2v^2) + \frac{B^2}{4\pi}\right]\frac{1}{\alpha}\frac{\partial v_x}{\partial t} + \left[(\rho + p)\gamma^4uv - \frac{\lambda B^2}{4\pi}\right]\times\frac{1}{\alpha}\frac{\partial v_z}{\partial t} + \left[(\rho + p)\gamma^2(1 + \gamma^2v^2) + \frac{B^2}{4\pi}\right]uv_{x,z} + \left[(\rho + p)\gamma^4uv - \frac{\lambda B^2}{4\pi}\right]uv_{z,z}$$
$$- \frac{B^2}{4\pi}(1 + u^2)b_{x,z} - \frac{B^2}{4\pi\alpha}[\alpha'(1 + u^2) + \alpha uu']b_x + \gamma^2u(\rho\tilde{\rho} + p\tilde{p})[(1 + \gamma^2v^2)v' + \gamma^2uvu'] + \gamma^2uv(\rho'\tilde{\rho} + \rho\tilde{\rho}' + p'\tilde{p} + p\tilde{p}')$$
$$+ \left\{(\rho + p)\gamma^4u[(1 + 4\gamma^2v^2)uu' + 4vv'(1 + \gamma^2v^2)] + \frac{B^2u\alpha'}{4\pi\alpha} + \gamma^2u(1 + 2\gamma^2v^2)(\rho' + p')\right\}v_x + \left\{(\rho + p)\gamma^2[(1 + 2\gamma^2u^2)(1 + 2\gamma^2v^2)v'\right.$$
$$\left. - \gamma^2v^2v' + 2\gamma^2(1 + 2\gamma^2u^2)uvu'] - \frac{B^2u}{4\pi\alpha}(\lambda\alpha)' + \gamma^2v(1 + 2\gamma^2u^2)(\rho' + p')\right\}v_z = 0 \quad (A10)$$

$$\left[(\rho + p)\gamma^2(1 + \gamma^2u^2) + \frac{\xi^2B^2}{4\pi}\right]\frac{1}{\alpha}\frac{\partial v_z}{\partial t} + \left[(\rho + p)\gamma^4uv - \frac{\xi B^2}{4\pi}\right]\times\frac{1}{\alpha}\frac{\partial v_x}{\partial t} + \left[(\rho + p)\gamma^2(1 + \gamma^2u^2) + \frac{\xi^2B^2}{4\pi}\right]uv_{z,z} + \left[(\rho + p)\gamma^4uv - \frac{\xi B^2}{4\pi}\right]uv_{x,z}$$
$$+ \frac{\xi B^2}{4\pi}(1 + u^2)b_{x,z} + \frac{B^2}{4\pi\alpha}[(\alpha\xi)' - \alpha'\xi + u\xi(u\alpha' + u'\alpha)]b_x + (\rho\tilde{\rho} + p\tilde{p})\gamma^2\left[a_z + uu'(1 + \gamma^2u^2) + \gamma^2u^2vv'\right] + (1 + \gamma^2u^2)(p'\tilde{p} + p\tilde{p}')$$
$$+ \gamma^2u^2(\rho'\tilde{\rho} + \rho\tilde{\rho}') + \left((\rho + p)\gamma^4\left\{u^2v'(1 + 4\gamma^2v^2) + 2v\left[a_z + uu'(1 + 2\gamma^2u^2)\right]\right\} - \frac{\xi B^2u\alpha'}{4\pi\alpha} + 2\gamma^4u^2v(\rho' + p')\right)v_x$$
$$+ \left((\rho + p)\gamma^2\left\{u'(1 + \gamma^2u^2)(1 + 4\gamma^2u^2) + 2u\gamma^2\left[a_z + (1 + 2\gamma^2u^2)vv'\right]\right\} + \frac{\xi B^2u}{4\pi\alpha}(\alpha\xi)' + 2\gamma^2u(1 + \gamma^2u^2)(\rho' + p')\right)v_z = 0 \quad (A11)$$

$$\frac{1}{\alpha}\gamma^2\rho\frac{\partial\tilde{\rho}}{\partial t} + \frac{1}{\alpha}\gamma^2p\frac{\partial\tilde{p}}{\partial t} + \gamma^2(\rho' + p')v_z + u\gamma^2(\rho\tilde{\rho}_{,z} + p\tilde{p}_{,z} + \rho'\tilde{\rho} + p'\tilde{p}) - \frac{1}{\alpha}p\frac{\partial\tilde{p}}{\partial t} + 2\gamma^2u(\rho\tilde{\rho} + p\tilde{p})a_z + \gamma^2u'(\rho\tilde{\rho} + p\tilde{p})$$
$$+ 2(\rho + p)\gamma^4(uV' + 2uva_z + u'v)v_x + 2(\rho + p)\gamma^2\left(2\gamma^2uu' + a_z\gamma^4 + 2\gamma^2u^2a_z\right)v_z + 2(\rho + p)\gamma^4uvv_{x,z} + (\rho + p)\gamma^2(1 + 2\gamma^2u^2)v_{z,z}$$
$$- \frac{B^2}{4\pi\alpha}\left[(v^2 + u^2)\xi\frac{\partial b_x}{\partial t} + (v^2 + u^2)\frac{\partial b_z}{\partial t} - \xi V(\xi v + u)\frac{\partial b_x}{\partial t} - u(\xi v + u)\frac{\partial b_z}{\partial t}\right] - \frac{B^2}{4\pi\alpha}\times\left[\xi(\xi v + u)v_{x,t} + (\xi v + u)v_{z,t} - (\xi^2 + 1)vv_{x,t}\right.$$
$$\left. - (\xi^2 + 1)uv_{z,t}\right] + \frac{B^2}{4\pi}(\xi\xi'v_z - \xi'v_x - \xi'vb_z + \xi'ub_x - vb_{x,z} + u\xi b_{x,z}) = 0 \quad (A12)$$